2014

Watershed Characteristics and Sediment PAH Contribution from Coal-Tar Sealant

EVAN DART
CE 394K
UNIVERSITY OF TEXAS AT AUSTIN

I. Introduction

The increase in urbanization in the United States has led to a drastic increase in sediment polycyclic aromatic hydrocarbons (PAHs) concentrations in urban lake sediments (Van Metre et al. 2000). PAHs are a suite of compounds that are produced during carbon combustion processes and are present in emissions and materials made from combustion byproducts (Van Metre and Mahler 2010). An increase in emissions and runoff from urban materials containing PAHs associated with increased urbanization has led to PAH accumulation in urban lake sediments (Van Metre et al. 2000).

In a subsequent study of the contribution of various PAH sources in urban environments to lake sediment PAH concentrations, coal-tar sealant was determined to be a significant contributor of PAHs to urban lake sediment PAH loadings with an average contribution of 50% of the total PAHs for 40 lakes in the United States (Van Metre and Mahler, 2010). Coal-tar sealant is a liquid sealant used to protect and beautify pavement, mainly parking lots and driveways (Van Metre and Mahler, 2010). Coal-tar sealant is highly concentrated in PAHs at about 5-10% by weight (Van Metre and Mahler, 2010). It is widely used, especially in the Eastern half of the United States and is one of the primary reasons for the stark increase in PAHs in urban lake sediments (Van Metre and Mahler, 2010).

PAHs enter urban waters and sediments primarily by particulate-association in runoff (Mahler et al. 2005). Coal-tar sealant is abraded by car tires and weathering over time and the particulates and associated PAHs from this abrasion are transported to urban stream and lake sediments via runoff (Mahler et al. 2005). As local watershed programs and municipalities become increasingly aware of the potential risk in the accumulation of PAHs in urban stream and lake sediments

(Crane 2014), more information and characterization is needed to determine the various factors that contribute to increased PAH concentrations in sediment.

The focus of this study was to determine the relationship between watershed characteristics and coal-tar sealant PAH contributions to sediment of various lakes around the United States. The lakes and associated watersheds were selected from the study by the USGS on sediment PAH concentration data for forty lakes and streams in the United States (Van Metre and Mahler 2010). Geospatial data and sealant PAH contribution were used to assess the relationship between watershed characteristics and PAH loadings in urban lake and stream sediments.

II. Methods

The lakes selected for this study were selected based on the contribution of PAHs in sediment by coal-tar sealant. Only lakes that had PAH contribution from coal-tar sealant were selected for this study. Twenty lakes from the study by the USGS were selected for the study (Figure 1).

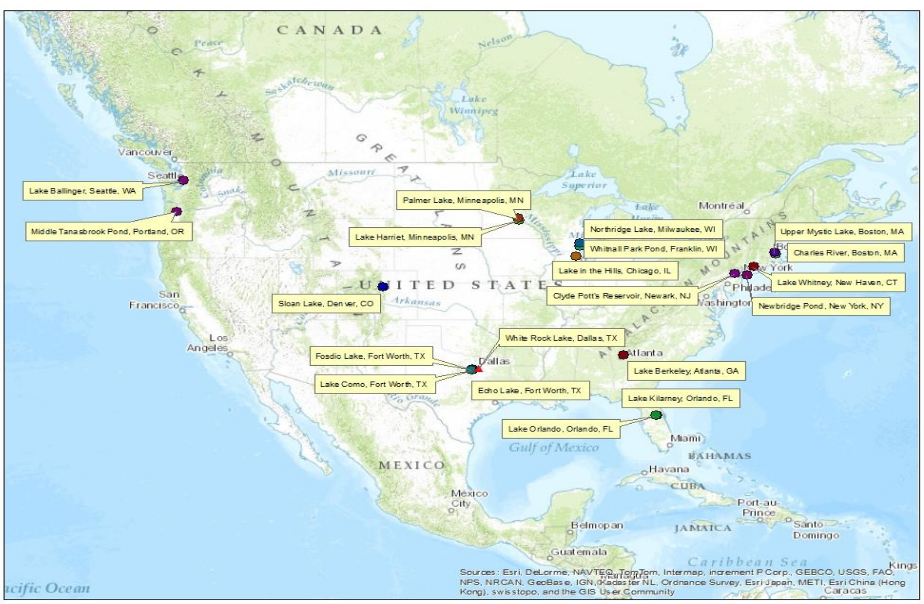

Figure 1. Selected Watersheds from the study by the USGS (Van Metre and Mahler 2010)

The geospatial data variables used in this study were selected based on their possible effect on runoff and runoff of pollutants. The variables selected were the average hydrologic slope, average stream network slope, impervious area fraction, and average annual rainfall. The average annual rainfall was selected based on the relationship between rainfall and runoff. The average hydrologic slope and average stream network slope were selected due to their effect on flow velocity, where slope increase is associated with an increase in flow velocity. The majority of PAHs in runoff are particulate-associated and the velocity of flow is a factor in the distance a particle will travel before settling (Gibbs et al. 1971). Impervious areas have a higher potential for runoff than other surfaces in catchment areas and the fraction of impervious area has been connected with increased urban pollutant runoff in watersheds (Arnold and Gibbons 1996). The method by which each of the geospatial data variables were calculated for each watershed are as follows.

Watershed Delineation

The watersheds were delineated using the National Elevation Dataset (NED 30m) from the ESRI servers, the National Hydrography Dataset Plus (NHDPlus) and the geoprocessing tools in ArcGIS. Location coordinates of the lakes were obtained from the supplementary information in the USGS study and the NHDPlus data was used to determine the location of the water bodies.

The watersheds were delineated in one of two ways. If the NHDPlus data was sufficient enough to provide a defined outlet of the water body of interest, the watershed tool was used and the outlet was defined as the juncture of the water body and the outlet stream of the water body (Figure 2). The elevation data from the NED 30m was also used to delineate the watershed.

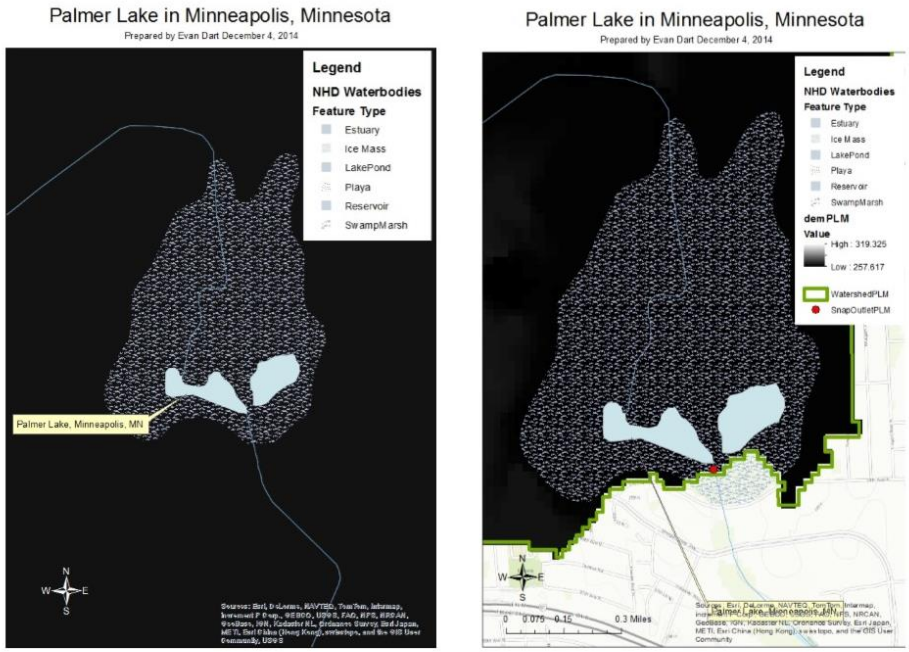

Figure 2. Watershed delineation using the NHDPlus defined outlet at Palmer Lake

However if the NHDPlus data did not provide a definite outlet stream of the lake, the watershed was defined by determining the cell with the lowest elevation at the edge of the water body. The watershed tool was then used with the outlet point defined as the cell with the lowest elevation at the edge of the water body.

Geospatial Data Extraction

The delineated watersheds were then used to extract geospatial data for each watershed from the national datasets. The digital elevation model (DEM) for each watershed was defined using the extract by mask tool to extract the elevation data for the basin of interest from the NED 30m layer (Figure 4).

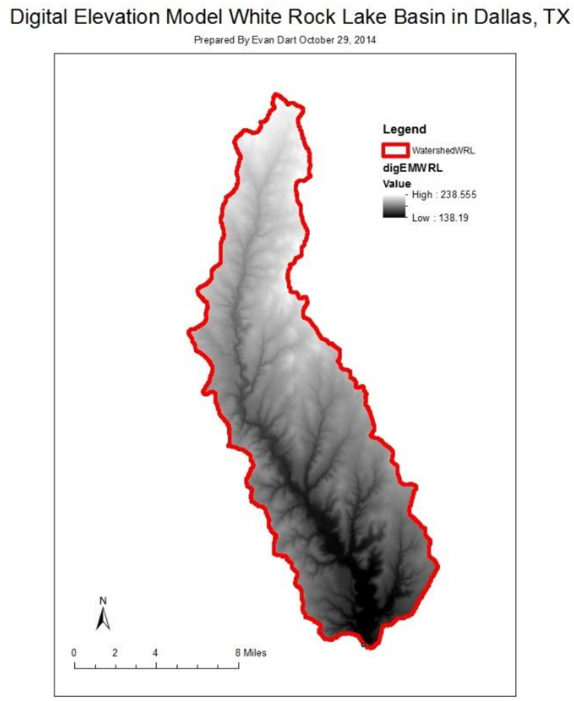

Figure 4. DEM Example: White Rock Lake Basin, Dallas, TX

The average annual rainfall for the watersheds was determined using the USA Mean Rainfall layer from the ESRI server. The extract by mask tool was used to extract the mean rainfall data from the national dataset to the watershed of interest for each watershed (Figure 5). The average annual rainfall in inches was then determined using the properties statistics of the extracted mean rainfall layer for each watershed (Figure 5).

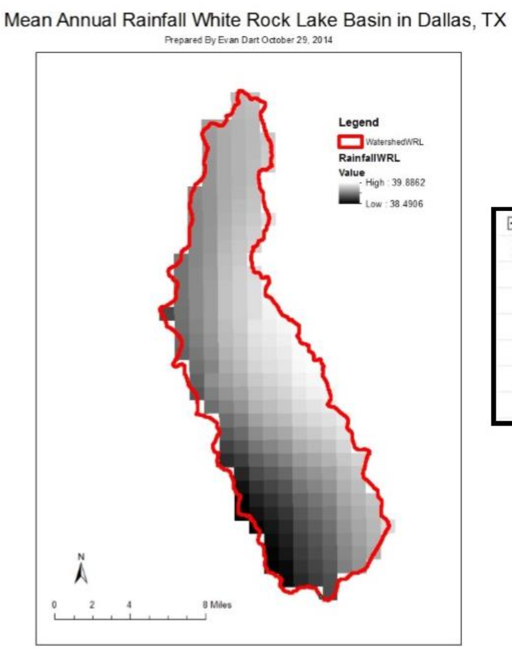

Statistics	
Band_1	
Build Parameters	
Min	38.49055099487305
Max	39.8862190246582
Mean	39.35954515596003
Std dev.	0.3112638533445018
Classes	0

Figure 5. Mean Annual Rainfall Example: White Rock Lake Basin, Dallas, TX

The impervious area fraction for each watershed was determined using the same extraction method used to determine the DEM and average annual rainfall, which was the extract by mask tool of the NLCD Impervious 2011 dataset using the watershed as the masking feature (Figure 6). The result of the extraction was an impervious dataset with each cell value in the raster representing an impervious area percentage from 1-100%.

The extract by mask tool eliminated the zero percent impervious value cells present in the national dataset, so the total cells in the extracted impervious raster did not represent the total area of the watershed. The fraction impervious had to be calculated using excel. The NLCD Land Cover dataset, which categorizes each cell as a certain type of land cover was used to determine the total number of cells within the watershed area, since both the Land Cover and Impervious datasets have the same cell size and overlap with each other (Figure 6).

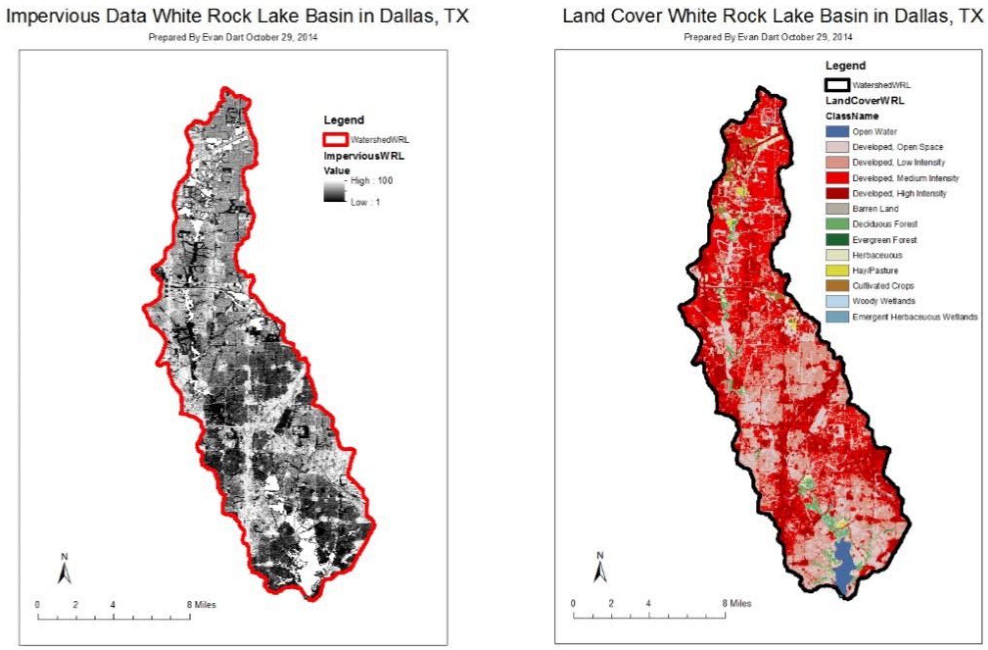

Figures 6. Impervious and Land Cover Examples: White Rock Lake, Dallas, TX

This total number of cells in the land cover raster for the watershed was then used to determine the impervious fraction of the watershed. The impervious fraction of each watershed was determined using the percent impervious value, cell count for each impervious value, and the total number of cells determined by the land cover raster for the watershed.

$$\% \, Impervious = \frac{\sum(i\% \, Impervious) \times (i \; Cell \; Count)}{Total \; Cell \; Count \; from \; Land \; Cover \; Layer}$$

The delineated watersheds were then analyzed based on each respective DEM. The watersheds were analyzed using a model to define the slope, aspect, flow direction, flow accumulation and percentage drop for the DEM of each watershed. The model was created in ArcGIS Toolbox Model builder (Figure 7).

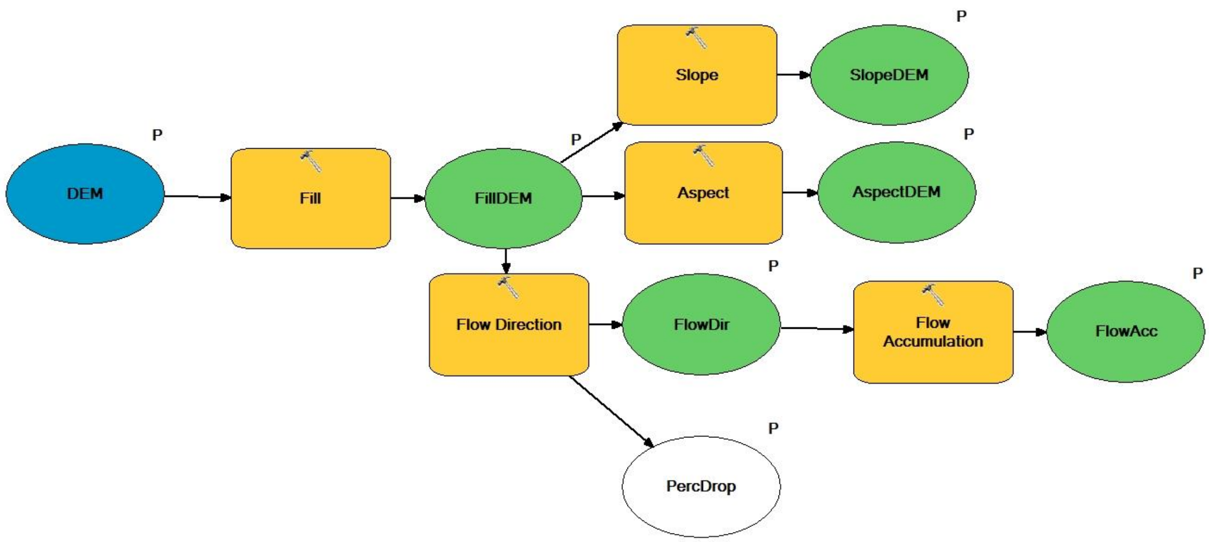

Figure 7. DEM Analysis Model

The outputs of the model were then used to further analyze the watershed. The model provides slope data for each cell in the watershed DEM. The average slope of each watershed was then determined from the properties statistics of the slope raster produced by the model (Figure 8).

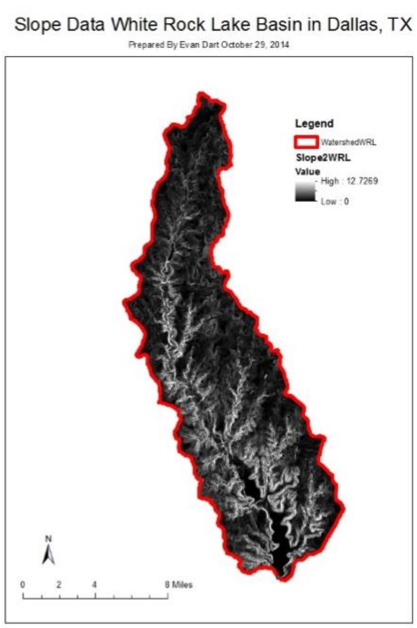

Statistics	
Band_1	
Build Parameters	
Min	0
Max	12.72685432434082
Mean	1.417639405001786
Std dev.	1.257171197571753
Classes	0

Figure 8. Slope Layer and Slope Statistics Example: White Rock Lake, Dallas, TX

The average slope of the stream network was determined by defining the stream network based on the flow accumulation layer and extracting the slope data for just the stream network. This was done via a model created in the ArcGIS Toolbox Model builder (Figure 9).

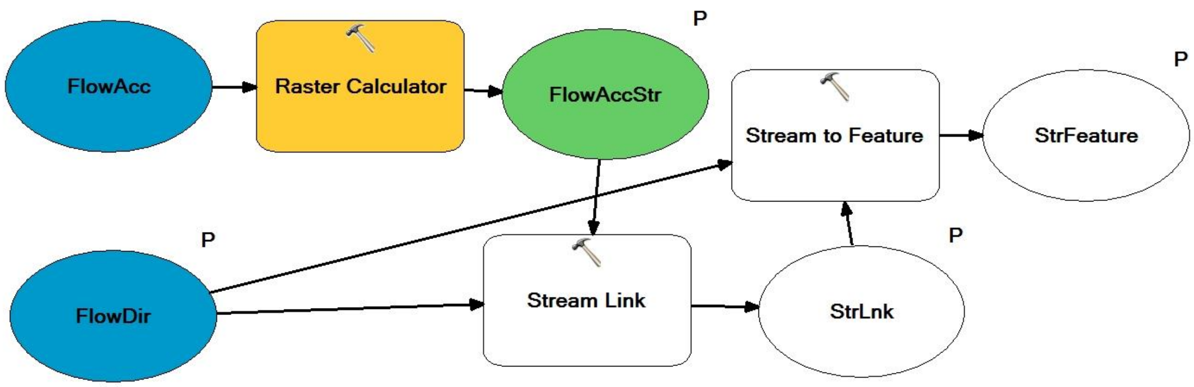

Figure 9. Stream Feature Model

The raster calculator was used to define the stream network for each watershed. The raster calculator was set to extract only the cells above a certain threshold of flow accumulation as defined by the flow accumulation raster output from the model. The threshold value varied for each watershed and was selected based on an observed, well-defined stream network after testing values in the flow accumulation raster calculation. The stream network was then defined using the stream link and stream to feature tools in ArcGIS.

After determining the stream feature for each watershed, the slope data for just the stream was extracted using the extract by mask tool using the slope layer as the input raster and the stream feature as the mask data (Figure 10). The average stream network slope was then determined using the properties statistics section of the new stream network slope layer (Figure 10).

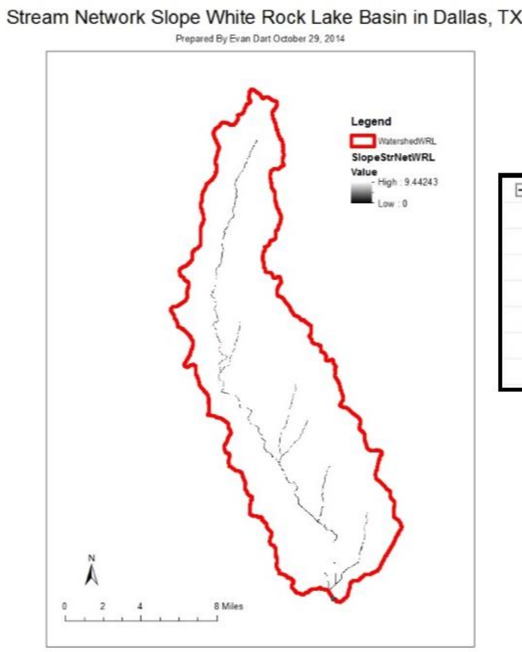

Statistics	
Band_1	
Build Parameters	
Min	0
Max	9.442431449890137
Mean	1.448359284067747
Std dev.	1.527825877816707
Classes	0

Figure 10. Stream Network Slope Layer and Statistics Example: White Rock Lake, Dallas, TX

The data was organized in a table representing the geospatial data extracted for all of the watersheds and used for further analysis (Appendix Table A-1).

III. Data Analysis/Discussion

Spearman's Rank Correlation Analysis

The relationship between the geospatial data collected for each watershed and the PAH contribution from sealant data was determined using Spearman's Rank Correlation analysis. Spearman's Rank Correlation analysis is a paired rank statistical method that determines the correlation between two variables (Reference). The association is measured by Spearman's Rank Correlation Coefficient, ρ

$$\rho = 1 - \frac{6\sum d_i^2}{n(n^2-1)}$$

where d_i is the difference in rank between the two variables analyzed for a specific watershed in this case, and n is the number of cases. Spearman's Rank Correlation Coefficient, ρ varies between -1 and +1, with a value of -1 indicating a strong negative correlation between the variables and a value of +1 indicating a strong positive correlation between the variables.

The analysis is done by ranking the value for each variable for a given watershed. After each value for each variable has been ranked, the difference in rank of the values of each variable for a given watershed, d_i is determined for further analysis. The difference in rank between the two variables being compared for each watershed is then inserted into the equation to determine the Spearman's Rank Correlation Coefficient between the two variables.

Table 1. Example Spearman's Rank Correlation Analysis with Stream Network Slope

Watershed	Sealant PAH Mass Contribution (mg/kg)	Rank	Mean Stream Network Slope	Rank	d_i	d_i^2
Lake Ballinger	11.830	10	1.269	9	1	1
Berkeley Lake	1.447	16	3.935	2	14	196
Charles River	48.931	3	1.076	12	-9	81
Echo Lake	2.856	15	1.743	5	10	100
Lake Harriet	20.712	9	0.543	17	-8	64
Lake Kilarney	46.490	4	0.197	19	-15	225
Lake Como	4.932	14	1.735	6	8	64
Lake Fosdic	9.344	11	1.417	8	3	9
Lake in the Hills	7.100	13	1.179	11	2	4
Upper Mystic Lake	55.978	2	1.184	10	-8	64
Newbridge Pond	56.961	1	0.503	18	-17	289
Clydespott Reservoir	1.117	19	3.664	3	16	256

Northridge Lake	27.007	6	1.039	13	-7	49
Lake Orlando	26.865	7	0.059	20	-13	169
Palmer Lake	24.021	8	0.818	16	-8	64
Sloan Lake	9.177	12	0.948	14	-2	4
Middle Tanasbrook Pond	0.804	20	4.568	1	19	361
White Rock Lake	1.268	18	1.448	7	11	121
Whitnall Park Pond	1.382	17	0.911	15	2	4
Lake Whitney	28.757	5	1.956	4	1	1

$$\rho = 1 - \frac{6\sum d_i^2}{n(n^2-1)} = -0.599$$

The reason the Spearman's Rank Correlation analysis was selected for the statistical analysis of the geospatial and PAH concentration data was because it does not require an assumption of a linear relationship between the two variables. Since it was not known what type of relationship the variables would have at the outset of this study, it was important not to eliminate any possible relationships with the statistical analysis.

The Spearman's Rank Correlation analysis was done for each geospatial data variable (average slope, average stream network slope, impervious fraction, and average annual rainfall) to assess their relationship with PAH data concentration. The geospatial data variables were all plotted against the PAH concentration data for each watershed in a scatter plot to give a visualization of the data (Figure.

Average Annual Rainfall and PAH Concentration Correlation Analysis

The correlation analysis for average annual rainfall and sediment PAH concentration attributed to coal-tar sealant resulted in a correlation coefficient of $\rho = 0.041$ (Figure 11).

Figure 11. Average Annual Rainfall – Sealant PAH Mass Contribution Scatter Plot

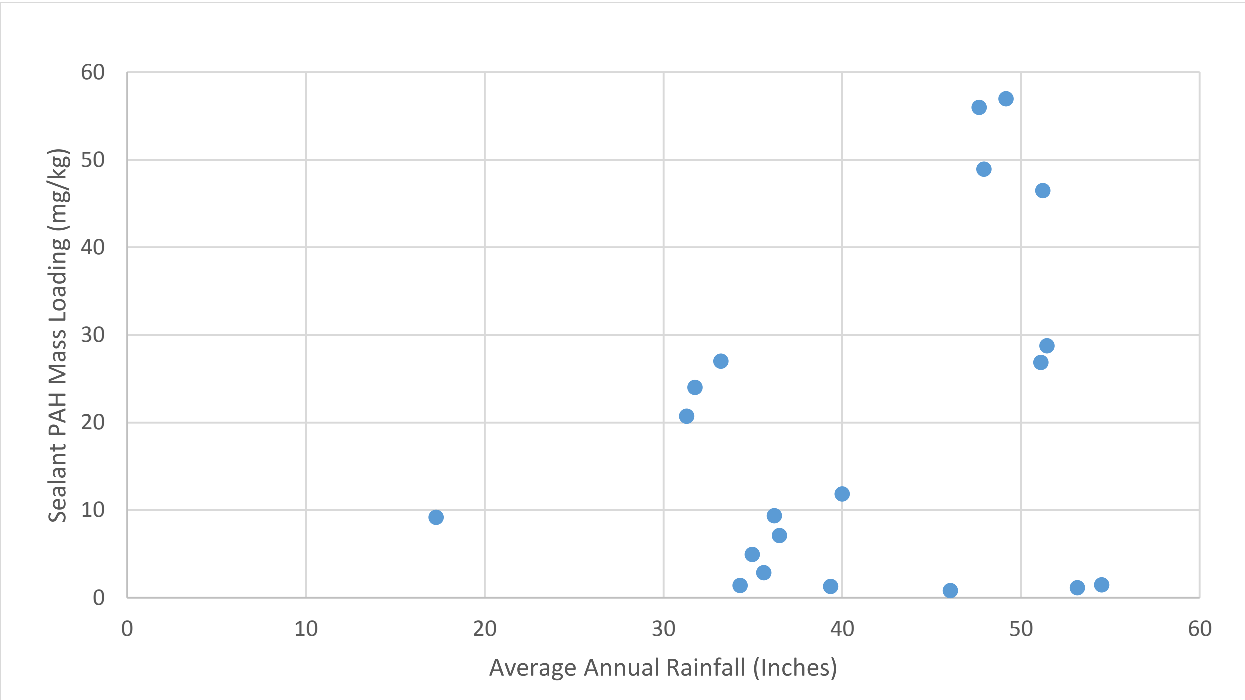

Spearman's Rank Correlation Coefficient, $\rho = 0.041$

The analysis revealed there is little correlation between average annual rainfall and the contribution of PAHs from coal-tar sealant for the corresponding watersheds. The correlation coefficient was also very close to zero, which indicates that a positive or negative trend in the relationship could not be established between the two variables. Some possible factors to explore in the role of rainfall in runoff of particulate associated PAHs is the intensity and frequency of rain events in the watersheds. The volume of runoff water and the velocity are factors in particulate transport from impervious surfaces and thus an intensity variable for rainfall in watershed would provide insight into the effects of rainfall on runoff of PAHs.

Fraction Impervious Area

The fraction impervious area correlation analysis with the sealant PAH contribution data resulted in little correlation between the variables, with a correlation coefficient ρ = 0.277 (Figure 12).

Figure 12. Impervious Fraction – Sealant PAH Mass Contribution Scatter Plot

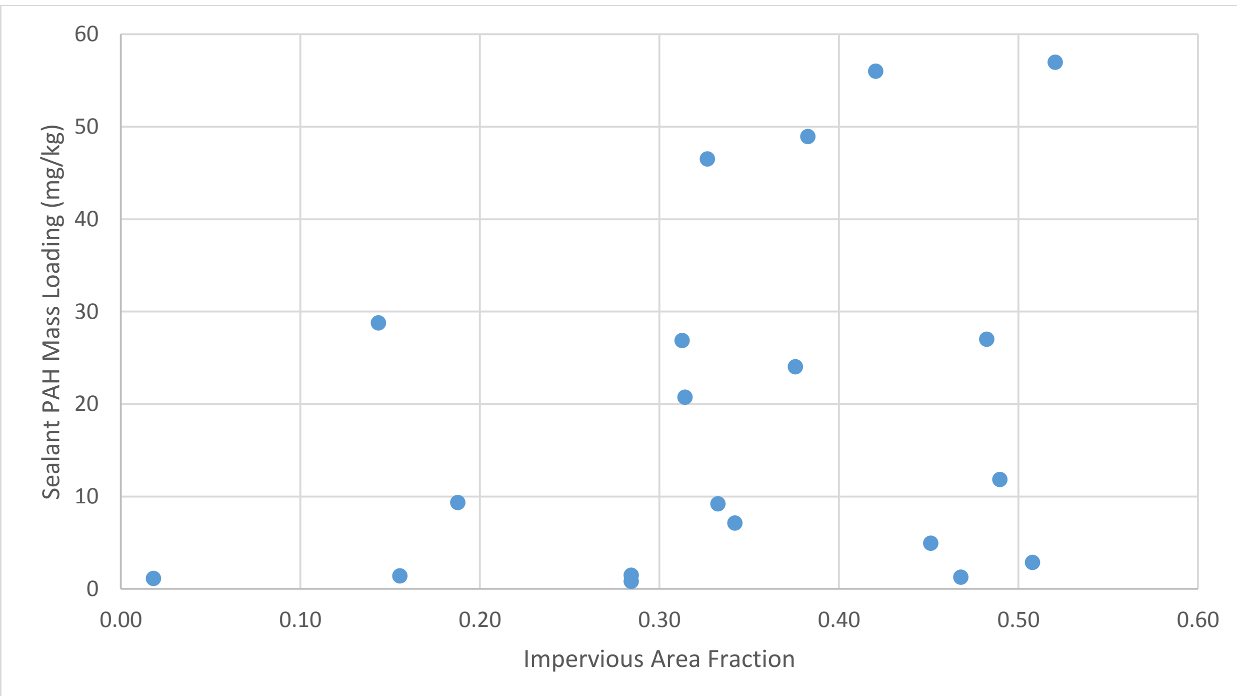

Spearman's Rank Correlation Coefficient, ρ = 0.277

The trend in the relationship indicates a positive, yet weak correlation between fraction impervious area in a watershed and the resulting PAH concentrations in the receiving water body sediment. The relationship indicates that a greater impervious area fraction may increase sealant contribution of PAHs. The trend result was expected since impervious area has a higher runoff potential than other surface types. Other factors to consider in further analysis would be the specific hydrologic routing from source areas and how much of the area in the runoff hydrologic route is impervious. This would require knowledge of the specific source areas which was not available for this study.

Average Hydrologic Slope of the Watershed

The average hydrologic slope and coal-tar sealant contribution of PAHs in sediment correlation analysis resulted in a correlation coefficient ρ = -0.418 (Figure 13).

Figure 13. Average Slope – Sealant PAH Mass Contribution Scatter Plot

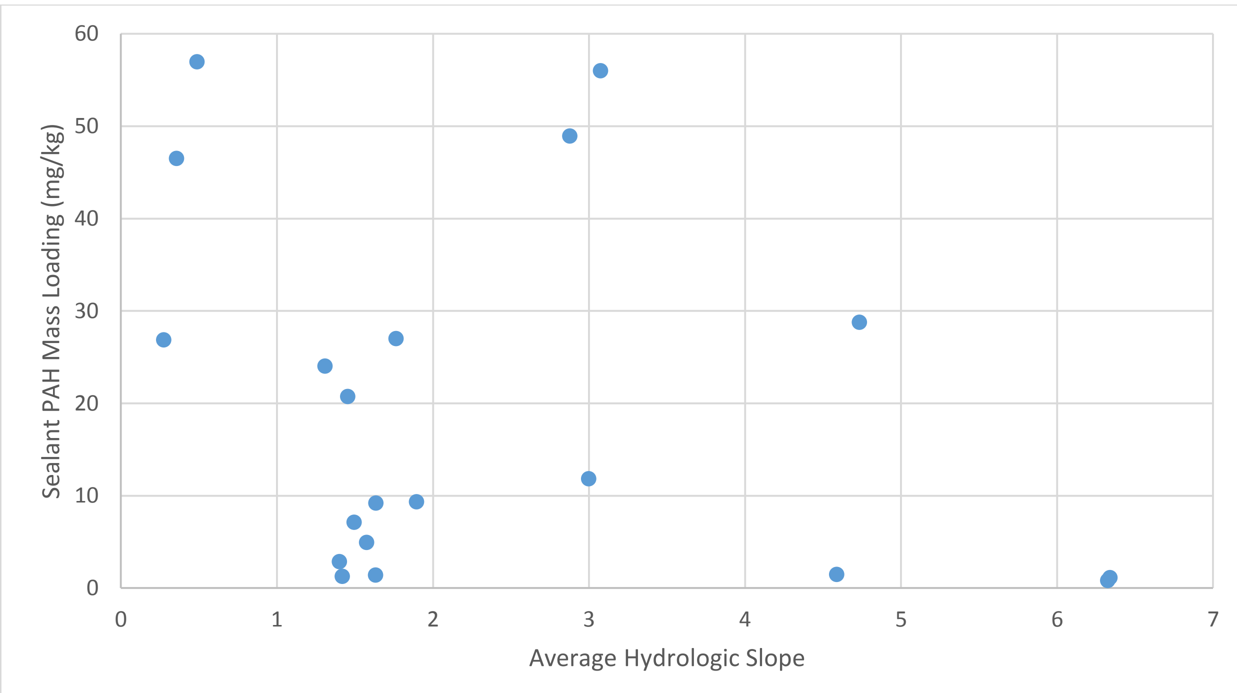

Spearman's Rank Correlation Coefficient, ρ = -0.418

This indicates a moderate correlation between the two variables. While it was expected that the average slope would have a positive correlation with the sealant PAH contribution data given the relationship between slope and runoff velocity, the correlation between slope and sealant PAH contribution was negative. It is possible that certain fluid dynamics phenomena and particle behavior in flow need to be considered in the correlation analysis. Particle size along with the type of flow (laminar or turbulent) determine the particle behavior and distance of travel in runoff (Guha 2008).

Average Stream Network Slope

The correlation coefficient for the average stream network slope and sealant PAH contribution statistical analysis was ρ = -0.599 (Figure 14).

Figure 14. Stream Network Slope – Sealant PAH Mass Contribution Scatter Plot

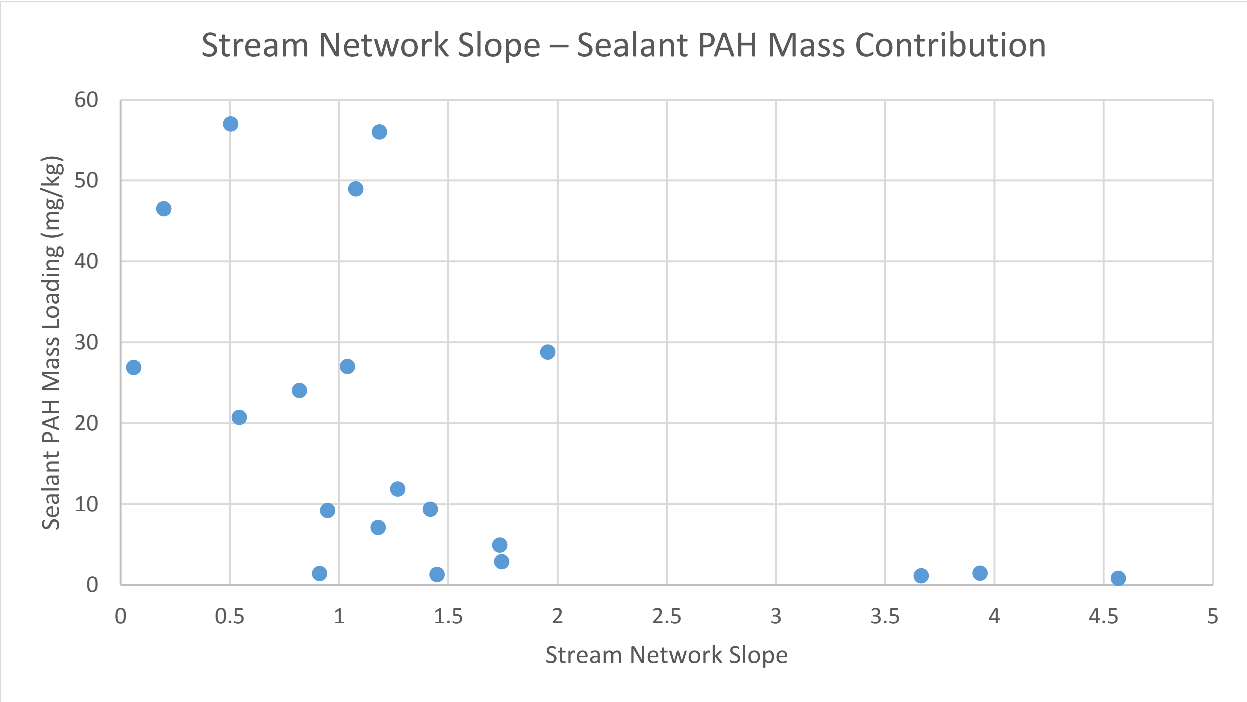

Spearman's Rank Correlation Coefficient, ρ = -0.599

The correlation analysis showed a negative, moderate correlation between the two variables. The correlation between the average stream network slope and sealant PAH contribution was the strongest correlation of the four geospatial data variables analyzed in this study. However the relationship was unexpectedly negative between the two variables, much like the average slope of the watershed. Based on the same principles of stream velocity and particulate travel distance as described with the average watershed slope, it was expected that the average stream network slope would have a positive correlation with sealant PAH contribution. The statistical analysis for the average stream network slope for the data analyzed proved the opposite trend was true. Much like the average slope analysis, it could be the case that there are certain particle properties and fluid dynamics principles that need to be considered for the correlation analysis in order to explain the deviation from the expected relationship between the two variables.

Conclusion

The intention of this study was to determine if certain watershed characteristics influence the contribution of PAHs from coal-tar sealant using a set of watersheds and associated PAH data. The statistical analysis done for each geospatial data variable revealed little correlation between the variables selected and the corresponding sealant contribution of PAHs for the selected watersheds. The classification of the relationship as positive or negative between the geospatial data and sealant contribution PAH data also revealed some unexpected results for the selected variables, mainly the average slope and average stream network slope.

The study would benefit from inclusion of more geospatial data variables that could affect runoff of particulate associated PAHs, since the variables selected did not show strong correlations with sealant contribution of PAHs in sediment. It is also possible that some of the results observed with the dataset were due to differences in the amount of sealant for each watershed. However, this information was not known for the study because geospatial data for coal-tar sealant was not available for the selected watersheds. Further studies including source characterization and quantification could provide more information on the effects of watershed characteristics on the transport of PAHs to receiving water bodies.

References

Arnold C, and Gibbons J. Impervious Surface Coverage: The Emergence of a Key Environmental Indicator. *Journal of the American Planning Association* 1996. 62:2, 243-258.

Crane, J. L. Source Apportionment and Distribution of PAHs, Risk Considerations, and Management Implications for Urban Stormwater Pond Sediments. *Archives of Environmental Contaminant Toxicology* 2014; 66: 176-200.

Gibbs R, Matthews M, Link D. The relationship between sphere size and settling velocity. *Journal of Sedimentary Research* 1971. 41:1, 7-18.

Guha, A. Transport and Deposition of Particles in Turbulent and Laminar Flow. *Annual Review of Fluid Mechanics* 2008. 40: 311-341.

Mahler B, Van Metre P, Bashara T, Wilson J, Johns D. Parking Lot Sealcoat: An Unrecognized Source of Polycyclic Aromatic Hydrocarbons. *Environmental Science and Technology* 2005. 39: 5560-5566.

Van Metre P, and Mahler B. Contribution of PAHs from coal-tar pavement sealcoat and other sources to 40 U.S. Lakes. *Science of the Total Environment* 2010; 409: 334-344.

Van Metre P, Mahler B, Furlong, E. Urban Sprawl Leaves Its PAH Signature. *Environmental Science and Technology* 2000; 34: 4064-4070.

Appendix

Table A-1. Geospatial Data and Rank Information for Selected Watersheds

			Rainfall			Slope			Impervious		Stream Network Slope			Sediment PAH Mass Contribution	
Watershed	City	State	Mean	Rank	STDEV	Mean	Rank	STDEV	Fraction	Rank	Mean	Rank	STDEV	Sealcoat	Rank
Lake Ballinger	Seattle	WA	39.99	10	0.174	2.998	6	2.491	0.490	3	1.269	9	1.498	11.830	10
Berkeley Lake	Atlanta	GA	54.51	1	0.030	4.587	4	3.152	0.284	16	3.935	2	2.944	1.447	16
Charles River	Boston	MA	47.92	7	0.808	2.876	7	2.669	0.383	8	1.076	12	1.640	48.931	3
Echo Lake	Fort Worth	TX	35.61	14	0.086	1.401	16	1.103	0.508	2	1.743	5	1.400	2.856	15
Lake Harriet	Minneapolis	MN	31.29	19	0.305	1.453	14	1.789	0.314	13	0.543	17	0.943	20.712	9
Lake Kilarney	Orlando	FL	51.23	4	0.034	0.356	19	0.396	0.327	12	0.197	19	0.345	46.490	4
Lake Como	Fort Worth	TX	34.97	15	0.057	1.574	12	1.513	0.451	6	1.735	6	1.581	4.932	14
Lake Fosdic	Fort Worth	TX	36.20	13	0.031	1.895	8	1.308	0.188	17	1.417	8	1.128	9.344	11
Lake in the Hills	Chicago	IL	36.49	12	0.070	1.494	13	1.310	0.342	10	1.179	11	1.409	7.100	13
Upper Mystic Lake	Boston	MA	47.66	8	0.237	3.073	5	3.094	0.420	7	1.184	10	1.746	55.978	2
Newbridge Pond	New York	NY	49.16	6	0.103	0.486	18	0.478	0.521	1	0.503	18	0.465	56.961	1
Clydespott Reservoir	Newark	NJ	53.16	2	0.078	6.339	1	4.328	0.018	20	3.664	3	2.712	1.117	19
Northridge Lake	Milwaukee	WI	33.21	17	0.024	1.763	9	1.460	0.482	4	1.039	13	1.158	27.007	6
Lake Orlando	Orlando	FL	51.11	5	0.047	0.274	20	0.441	0.313	14	0.059	20	0.132	26.865	7
Palmer Lake	Minneapolis	MN	31.76	18	0.291	1.307	17	1.743	0.376	9	0.818	16	1.424	24.021	8
Sloan Lake	Denver	CO	17.29	20	0.357	1.633	10	1.005	0.333	11	0.948	14	0.798	9.177	12
Middle Tanasbrook Pond	Portland	OR	46.04	9	5.392	6.324	2	5.543	0.284	15	4.568	1	4.488	0.804	20
White Rock Lake	Dallas	TX	39.36	11	0.311	1.418	15	1.257	0.468	5	1.448	7	1.528	1.268	18
Whitnall Park Pond	Milwaukee	WI	34.28	16	0.039	1.631	11	1.586	0.155	18	0.911	15	1.024	1.382	17
Lake Whitney	New Haven	CT	51.46	3	0.706	4.734	3	4.913	0.144	19	1.956	4	2.469	28.757	5